CHAPTER 12

The Origin of Electromyograms - Explanations Based on the Equilibrium Point Hypothesis

A. G. Feldman, S. V. Adamovich, D. J. Ostry and J. R. Flanagan

12.1 Introduction

In the present chapter, we review and further develop the equilibrium-point (*EP*) hypothesis or λ model for single and multi-joint movements (Feldman 1974, 1986; cf. Chapters 11, 13-22). A departure point is the notion of the measure of the central control signals underlying movement production. According to the *EP* hypothesis, central commands parameterize the threshold of motorneuron (*MN*) recruitment. The usual assumption that central signals are directly associated with muscle activation, i.e. recruitment of *MN*s and their firing frequencies, is rejected (see also Bernstein, 1967). This assumption ignores the role of muscle afferents in motor control as well as the non-linear threshold properties of *MN*s. In this chapter, we discuss electromyographic (*EMG*) patterns of single- and multi-joint movements in terms of the *EP* hypothesis. Reference will be made to the central control signals which set the inter-muscular interaction (cf. Nichols, 1989) as well as to the concept of muscle activation area which is essential for the explanation of the *EMG* patterns.

It is necessary to make an initial remark concerning the understanding of the *EP* hypothesis. A ***static*** arm position is associated with an equilibrium state of the corresponding spinal and supraspinal systems, including peripheral afferent systems, muscle properties, and external forces (loads). This static state is achieved by the dynamic interaction of these subsystems. The *EP* hypothesis suggests that the *CNS* can alter the equilibrium state at the spinal level by changing specific neurophysiological parameters. Subsequently, the *CNS* initiates ***dynamic*** processes which force the subsystems to find a new equilibrium. Changes in muscle activation and forces as well as limb movement itself are a reflection of the dynamic processes associated with the transfer of the neuro-biomechanical system from one equilibrium state to another. The final equilibrium state essentially depends on the parameters the *CNS* specifies as well as on the external load. It should be emphasized that muscle activation by way of the recruitment or derecruitment of motor units occurs as a ***consequence*** of the disturbance of the initial equilibrium state at the neuronal level. Neither the timing nor the magnitude of the muscle activation ("*EMG* bursts") have to be programmed for the execution of the movement, just as muscle elastic properties, forces and kinematic variables do not appear to be preplanned or calculated in the course of movement. Therefore, the *EP* hypothesis can be considered as an alternative to the notion that the *CNS* preplans movement kinematics and performs inverse-dynamic computation in the course of movement to generate appropriate muscle activation and forces (see Hollerbach, 1985).

The *EP* hypothesis suggests a more primary reason for biological movements than merely a change in muscle forces or, indeed, even muscle activation. In contrast, muscle activation is considered to be the basic mechanism in shifts of the limb equilibrium in an alternate version of the *EP* hypothesis [Bizzi, 1980; Hogan, 1984; for discussion see Chapters 11 (Hogan and Winters) and 17 (Flash)]. But, in essence, the cause and effect of movement production are inverted in this version of the original formulation (Feldman, 1974, 1986).

Multiple Muscle Systems: Biomechanics and Movement Organization
J.M. Winters and S.L-Y. Woo (eds.), © 1990 Springer-Verlag, New York

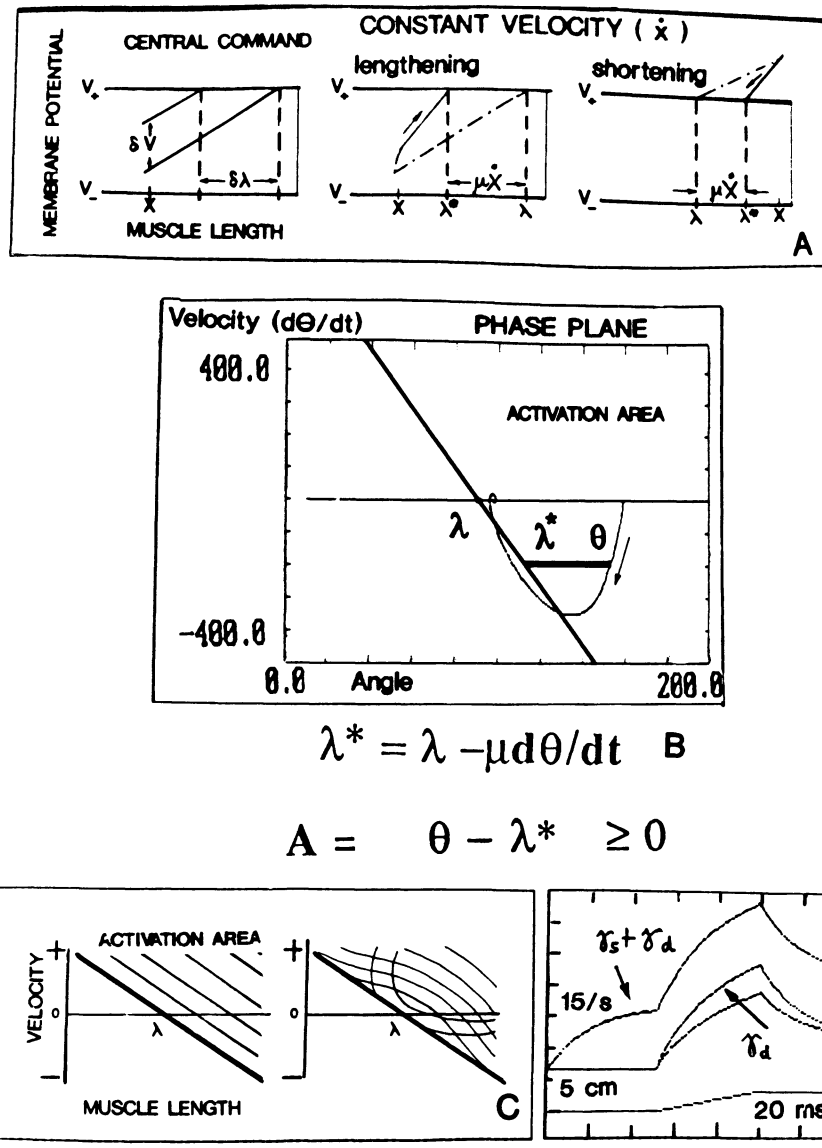

Figure 12.1: The muscle activation area and its properties. *A) Left panel:* Two equivalent measures (δV and $\delta\lambda$) of central control signals. V_-, V_+ are minimum and maximum threshold membrane potentials of the motoneuron. If control signals are constant, membrane potential (V) increases with muscle length, x (solid inclined lines). λ is the static threshold length for motoneuronal recruitment. *Right panels:* Dynamic threshold length (λ^*) decreases with velocity (dx/dt). Trajectories of the membrane potential are shown for statics (dashed-pointed lines) and dynamics (solid lines). μ is the damping coefficient for dx/dt. *B)* Muscle activation area in angular coordinates. The solid line is the border of the *MAA*. The horizontal bar is a measure of muscle activation, *A*. A simulated phase trajectory for fast active movements is shown. *C)* Two examples of the inner structure of the *MAA* with a stable (left) and a variable (right) order of the motoneuronal recruitment as a function of velocity. *D)* Modelled responses of muscle spindle afferents to a ramp muscle stretch and stimulation of gamma static (γ_s) and dynamic (γ_d) efferents.

12.2 Basic Concepts and Mathematical Equations

12.2.1 Muscle Activation Area (*MAA*)

A constituent part of the *EP* hypothesis is the concept of *MAA* (Feldman, 1974, 1986) which integrates, in a compact form, the non-linear properties of α *MN*s, the effects of afferent influences and descending central commands to α, β, γ *MN*s, and the effects of interneurons mediating afferent and efferent inflows to α *MN*s. The properties of specific phasic and tonic reflexes (the tendon reflex, unloading reflex, stretch reflex) are also integrated in the concept.

Statics

Consider a single α *MN* with intact afferent and efferent connections. Let V be an initial, subthreshold membrane potential of the *MN* at an initial muscle length, x, when descending control signals are fixed. Now let us suppose that the *CNS* specifies a new magnitude of the tonic control signal. The effect can primarily be measured by a decrement (δV) in the membrane potential (Fig. 12.1a, left panel). The decrement results from both direct influences of the signals on the *MN* and indirect influences mediated by β and γ *MN*s, muscle spindle afferents, and interneurons. A quasi-static stretch of the muscle from the initial length results in increasing depolarization as a function of x because of the proprioceptive feedback. The threshold membrane potential (V_+), and consequently the recruitment of the *MN*, will be reached at a muscle length λ_1 if the central command is absent and at a muscle length λ_2 if the central command (δV) is present. Thus, the command is expressed as a decrement ($\delta\lambda$) of the threshold muscle length at which the *MN* is recruited (Figure 12.1a). Motoneuronal activation in statics occurs when:

$$x - \lambda > 0 \tag{12.1}$$

where x is associated with the actual muscle length and λ with the threshold muscle length. In the suprathreshold area, motoneuronal firing is an increasing function of $x - \lambda$.

Each *MN* has its own threshold λ_i, and all thresholds are interrelated so that:

$$\lambda_i = f_i(\lambda) \tag{12.2}$$

where $\lambda = \lambda_1$ is the threshold of the *MN* which is recruited first. According to Burke et al. (1976), motor units are recruited in the order of *S*, *FR*, and *FF* where *S* are slow, fatigue-resistant motor units, *FR* are fast, also fatigue resistant, and *FF* are fast, fatiguable motor units. In the suprathreshold area (*Eq. 12.1*), muscle activation, A (i.e. the number of active *MN*s and their firing frequencies), is an increasing function of the difference between x and λ. For the purpose of simplicity, muscle activation will be directly associated with this difference if $x \geq \lambda$ and 0 if $x < \lambda$:

$$A = x - \lambda \tag{12.3}$$

Invariant Characteristics (ICs)

The static muscle torque, T, is a function of muscle activation such that $T = f(x - \lambda)$. When λ is constant, muscle torque depends only on the muscle length. We call this dependence the invariant characteristic (*IC*). It should be emphasised that the *IC* of the muscle including feedback is not equivalent to the torque-position function obtained when the muscle is deprived of feedback and stretched under constant level of activation. A given *IC* may be characterized by a single threshold; however, muscle activation varies as a function of length.

Dynamics

In dynamics, if the muscle is stretched at a speed, dx/dt, the muscle spindle afferents produce an additional speed-dependent component of activity which gives rise to an additional depolarization of the *MN*. As a result, the threshold V_+ will be reached at a muscle length (λ^*) which is less than the static threshold length, λ (Figure 12.1A, middle panel). On the other hand, if the *MN* has been recruited, muscle shortening can lead to de-recruitment. In this case, the dynamic threshold length, λ^*, also depends on the speed of shortening and is greater than the static threshold length (Figure 12.1A, right panel). On the whole, the threshold λ^* is a decreasing function of speed dx/dt:

$$\lambda^* = \lambda - dx/dt \tag{12.4}$$

where μ is a coefficient having the dimension of time. Note that muscle shortening is considered negative. *Eq. 12.3* for muscle activation is

modified for dynamic conditions correspondingly:

$$A = x - \lambda^* = x + dx/dt - \lambda \qquad (12.5)$$

The above relations can be represented in a simple graphical form (Figure 12A,B). The boundary condition $x - \lambda^* = 0$ represents a straight line in a phase plane (i.e. muscle length x versus speed dx/dt; see also Chapter 13 (Wu et al.). The *MAA* is the part of the plane to the right of the line. The position of the line (determined by the λ) can be modified by central commands as discussed above. The slope is associated with the coefficient μ of velocity (*Eq. 12.4*) and reflects the dynamic sensitivity of muscle spindle afferents (see below). The sensitivity is specified by activity of γ dynamic and β *MN*s. Consequently, it also can be modified by central commands. The level of muscle activation is measured by the horizontal distance between the threshold line and the point (x, dx/dt), which represents the current combination of the kinematic variables. The *MAA* can also be represented in corresponding angular variables (Figure 12.1B). In this case parameter λ is the threshold joint angle for recruitment of *MN*s of the corresponding muscle.

A single-joint movement can be represented as a trajectory on the phase plane. If the trajectory enters the *MAA*, muscle activity arises and increases as the trajectory goes deeper into the area. When the trajectory leaves the area, muscle activity disappears. In particular, Figure 12.1B shows a final position of the border of the flexor *MAA* and the trajectory for a fast flexor movement. It can be seen that the trajectory leaves and then reenters the *MAA*. Thus, flexor activation is predicted to be bi-phasic in this fast movement. The muscle activations and de-activations occur after time delays but in the present model these delays were not included.

Inside the *MAA* there are threshold lines for different *MN*s (Figure 12.1C) so that the area has a definite inner structure ("landscape") which allows, in principle, the prediction of the number of active motoneurons and their firing rates as a function of control and kinematic variables. Unfortunately, the structure of the *MAA* is not fully understood and further experimental work is required to map out the *MAA* in detail.

We may consider theoretical examples of the inner structure of the *MAA* with special reference to the problem of ordered or selective recruitment of MNs. In Fig. 12.1C (left panel), the threshold lines of *MN*s do not cross each other. In this case, the order of motoneuronal recruitment (*S*, *FR*, *FF*) remains the same irrespective of the method of muscle activation (changes in variables x and dx/dt or control parameters λ and μ). However, reversals in recruitment order are known to exist. In this case, individual threshold lines will cross each other. One possibility is shown in Figure 12.1C (right panel), in which the order of recruitment is speed dependent. The recruitment order of MNs also differs with respect to fatigue. This suggests that the structure of threshold lines in the MAA is non-stationary (i.e., time-dependent).

The above analysis shows that reversals in the order of recruitment of *MN*s are not necessarily associated with the use of specific central inputs to *MN*s. The intrinsic, synaptic organization of the motoneuronal pool, as well as the properties of MNs themselves, can give rise to the reversals. This is consistent with the idea that the activity of a motoneuronal pool is a function of one integral variable, $x - \lambda^*$, as has been suggested in *Eq. 12.5*.

12.2.2 Muscle Spindles

Static and dynamic properties of muscle spindles and their effects on *MN*s have been integrated in the concept of the *MAA*. Consider, however, muscle spindle properties in more detail (cf. Chap. 13), with the purpose of further developing the concept of the *MAA*. We suggest the following differential equation for the firing frequency (*S*) of muscle spindle afferents:

γ static γ dynamic & β *MN*s
$\downarrow$ $\downarrow$

$$S + c\,dS/dt = a(x - l) + b\,dx/dt \qquad (12.6)$$

The first term on the right side of the equation is a static length-dependent component of activity of muscle spindle afferents. The second term is the dynamic speed-dependent component. The arrows indicate the parameters controlled by γ static, γ dynamic, or β *MN*s. An increase in the tonic component of muscle spindle activity is associated with activation of γ static *MN*s and, as a result, with a decrease in the parameter l. The coefficient

b represents the dynamic sensitivity of spindle afferents. It can be modified by γ dynamic and β *MN*s. The coefficient a is the spindle afferent positional sensitivity. The fact that the sensitivity is different for short and large lengthenings [e.g. see Chapter 13 (Wu et al.)] can be taken into account if we assume that a is an appropriate function of lengthening, δl. The second term on the left-hand part of *Eq. 12.6* is associated with decay in spindle primary afferent activity after the end of muscle stretch which is presumed to be exponential with a time constant c. *Eq. 12.6* reproduces typical responses of muscle spindle afferents to ramp stretch as well as the effects of stimulation of γ static and γ dynamic *MN*s (Figure 12.1D).

During muscle stretch at a constant speed the speed-dependent component of the spindle primary response has the form $b\ dx/dt - c\ dS/dt = (b - c\ a)\ dx/dt$, where S is derived from *Eq. 12.6*. This component is less than the speed-dependent response $b\ dx/dt$ (*Eq.12.6*) in the absence of decay. Houk and Rymer (1981; see also Chapter 13 (Wu et al.)) have indicated that the gain of muscle spindle afferent responses to velocity can be low during constant velocity stretch. Our model shows that the gain is equal to $b - ca$, i.e. it can be low due to decay while the actual dynamic sensitivity of the afferents to velocity remains high. Thus, in contrast to Houk and Rymer (1981), we see no reason for postulating a complex non-linear dependence of muscle spindle activity on velocity.

Now let us use *Eq. 12.6* to further develop the concept of *MAA*. We assume that spindle afferent signals are transformed linearly to the motoneuronal membrane potential V:

$$V = g\,S + e \qquad (12.7)$$

where g is the gain of the transformation ("the weight" of synaptic transmission) and e is the component of membrane potential associated, in particular, with direct central inputs to *MN*s not depending on the spindle afferent transmission. Notice that the condition of motoneuronal recruitment, $V = V_+$, can be observed in dynamic conditions when $x = \lambda^*$ or in static conditions when $x = \lambda$ but dx/dt and dS/dt equal zero. It follows from *Eqs. 12.6* and *12.7* that:

$$\lambda^* = \lambda - \mu'\ dx/dt + (c/a)\ dS/dt \qquad (12.8)$$

where $\mu' = b/a$ is the ratio of dynamic to positional sensitivity for spindle afferents. It can be seen that the threshold of muscle activation has a time-dependent component due to the decay of spindle afferent activity. Geometrically, this suggests that the boundary line of *MAA* can be shifted by central control signals or by decay of spindle afferent discharge. Consequently, the boundary line can move even though the central control signals are fixed. *Eq. 12.5* for the magnitude of muscle activation remains but *Eq. 12.4* for λ^* is replaced with *Eq. 12.8*.

Eq. 12.6 for muscle spindle firing must be modified to be consistent with the fact that muscle spindle afferent activity temporarily disappears during a twitch contraction of the muscle under isometric conditions – a standard test for spindle afferents. To reproduce this effect, it is necessary to take into account the interaction of the contractile and the series elastic components of the muscle. To do so, the length of the whole muscle (x) in *Eq. 12.6* must be replaced with the length of its contractile component (x_c). The same holds for all equations related to the *MAA*.

12.2.3 Angular Variables

While considering the co-ordination of activity of flexor and extensor muscles of a joint, it is convenient to use angular variables (joint angle θ, angular velocity $\omega = d\theta/dt$, etc.) instead of linear ones (x, v, etc.). Flexor length increases and extensor length decreases with increases of joint angle. The symbol λ will now refer to threshold angle: λ_1 for flexor muscles and λ_2 for extensors. In addition, invariant characteristics (*IC*s) will refer to muscle torque/angle functions associated with a constant value of threshold angle λ. The transformation from angular to linear variables may be linearly approximated by $x = m\theta + n$ where m is associated with the muscle moment arm about the joint. The sign of m is opposite for flexor and extensor muscles. Note that the form of *Eqs. 12.4*, *12.6*, and *12.8* is unaffected by this substitution. The condition of activation for the flexor and extensor muscles in angular variables is given by:

$$A_1 = \theta - \lambda_1^* \geq 0; \quad A_2 = \lambda_2^* - \theta \geq 0 \qquad (12.9)$$

where λ_1^* and λ_2^* are dynamic threshold angles for activation of the flexor and extensor muscles, respectively.

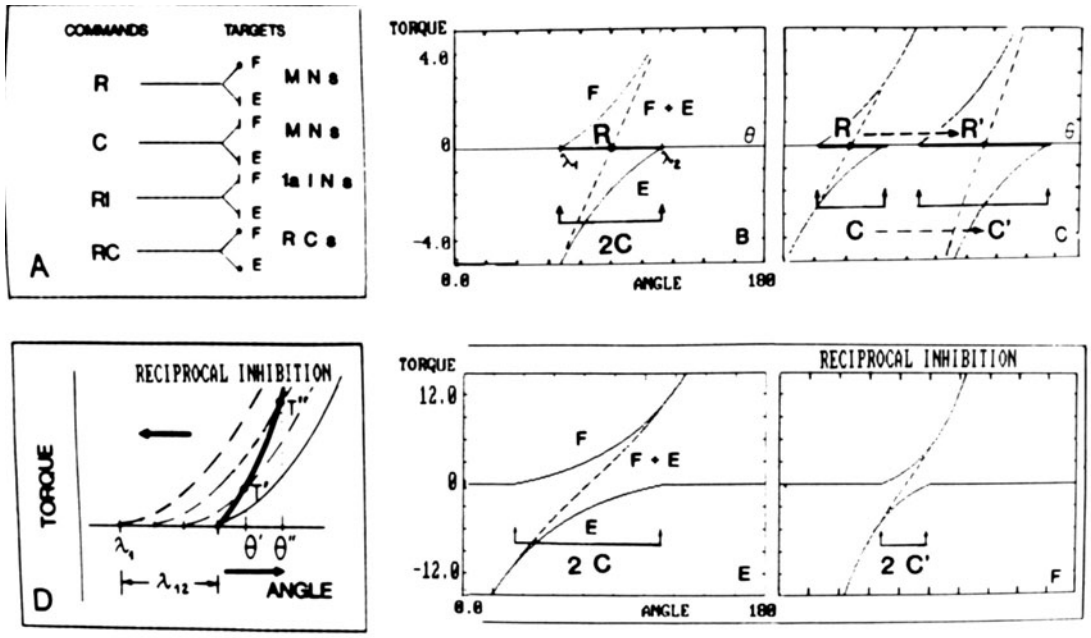

Figure 12.2: Central commands and intermusclar interactions in the λ model. ***A)*** neurophysiological schemes for the commands. *F MNs* and *E MNs* are flexor and extensor motoneurons; inhibitory synapses are marked with filled circles (see Sections 12.2 and 12.3). ***B, C)*** *R* and *C* commands in terms of shifts of the invariant torque/angle characteristics (ICs). ***D-F)*** Reciprocal inhibition of antagonist muscles increases the slope of the agonist *IC* and decreases the size of the coactivation area for flexor and extensor muscles.

12.2.4 Central Commands

It is suggested that high brain levels control flexor and extensor muscles as a coherent unit, but there exist a variety of coherent commands (Figure 12.2A) that allow the nervous system to set any combination of flexor-extensor activity (Feldman, 1980). According to the λ model, however, each central command is primarily expressed not in terms of muscle activations but in terms of λ_1 and λ_2. Nevertheless, the names of the commands reflect their typical (but not necessarily universal) effects on flexor and extensor activity: reciprocal (*R*), coactivation (*C*), reciprocal inhibition (*RI*), and Renshaw inhibition (*RC*) commands.

We first review the definition of the *R* and *C* commands (Feldman, 1980). The effects of the interaction of agonist and antagonist muscles mediated by specific afferents and spinal interneurons (e.g., those of reciprocal inhibition) will be considered later in this chapter.

C Command

If $\lambda_2 > \lambda_1$ (Figure 12.2B), the muscles work together in the range $\lambda_1 < \theta < \lambda_2$. Summation of the flexor and extensor torques in this coactivation range gives rise to the total *IC* of the joint (dashed line). The slope (stiffness) of the total *IC* exceeds that of either individual *IC*. The coactivation range expands with the difference between the thresholds. Thus, $C = (\lambda_2 - \lambda_1)/2$ provides a measure of the specific coactivation command. Its modification from *C* to $C\hat{I}$ (Figure 12.2C) results in a greater distance between flexor and extensor *IC*s and gives rise to a change in the slope of the total *IC*. Note that the *C* and *R* commands are independent such that the coactivation area may vary without shifting the position *R*. For simplicity, we have assumed that the flexor and extensor *IC*'s are the same form. Thus, equal but opposite shifts of these *IC*s will not affect *R*. An additional effect of the command *C* is a linearization of the total *IC*. If $\lambda_1 > \lambda_2$, the operational range of joint angles attainable *in situ* has three zones in which either one of the muscles or none of them is active. The absence of coactivation range can be considered a negative coactivation: $C < 0$, in which case the term total *IC* may also be used. The total *IC* consists then of a flexor and an extensor *IC* situated apart.

R Command

Now consider a command $R = (\lambda_2 + \lambda_1)/2$. Since the form of flexor and extensor *IC*s is assumed to be identical, the R coincides with the joint angle at which the total *IC* crosses the θ-axis if $C > 0$ (Figure 12.2B). This command can be associated with the position of the total *IC* on a torque/angle plane. At the same time, if the external load at the joint is zero, the R coincides with the equilibrium position of the joint. To modify this position from R to $R\hat{I}$, the two individual *IC*s have to be shifted in the same direction (Figure 12.2C). Physiologically, this command may be elicited by descending central signals with reciprocal effects on flexor and extensor *MN*s (Figure 12.2A) and thus is called the reciprocal command (Feldman, 1980). Its modification shifts the total *IC* and the equilibrium position. Consequently, the limb moves to the new position. Damping of the system to avoid oscillations is provided by velocity dependent activity of muscle spindle afferents and the mechanism of muscle contraction [see below and Chapter 5 (Winters) on force–velocity relation].

12.3 Intermuscular Interactions

Muscle spindle afferents have mono- and polysynaptic connections with homonymous and heteronymous *MN*s. We will describe in terms of the λ model the intermuscular interactions between *MN*s of synergist, agonist and antagonist muscles mediated by muscle afferents.

12.3.1 Reciprocal Inhibition (*RI*) of Antagonist Muscles

The system of *RI* between flexor and extensor *MN*s has been studied in detail (Hultborn, 1972; Nichols, 1989). It is active during natural movements in man and animals (Feldman and Orlovsky, 1975; Baldissera et al., 1981). *Ia* interneurons (*Ia IN*s) mediating *RI* are controlled by descending pathways (Grillner, 1975; Lundberg, 1982) and receive effective inhibitory inputs from Renshaw cells (Hultborn, 1972) and excitatory inputs from antagonist muscle spindle afferents.

From a theoretical point of view, it is important to find an adequate measure of *RI*. It is clear that the effects of *Ia IN*s are not necessarily expressed in terms of a decrease in the activity of antagonist *MN*s: the inhibitory action of *Ia IN*s can be subthreshold but not negligible, which can affect the timing and magnitude of future activity of antagonist *MN*s.

It has been shown that the stretch reflex threshold of the gastrocnemius muscle in the decerebrated cat increases if its antagonist lengthens (Feldman and Orlovsky, 1972). In other words, the *RI* effect can be measured by a shift in the threshold length of the extensor muscle, under the influence of spindle afferents of the flexor muscle and vice versa. Consequently, we hypothesize that the flexor reflex threshold angle λ^*_1 is modified by a value $\lambda^*_{12} > 0$ conditioned by extensor spindle afferent activity S_2 so that the new threshold angle is given by

$$\lambda^*_1 = \lambda^*_1 + \lambda^*_{12} \tag{12.10}$$

where λ^*_{12} is an increasing function of S_2. The same effect occurs for the extensor muscle as the interaction between flexor and extensor *MN*s is mutually inhibitory (Hultborn, 1972). Note that the form of relationship also holds for statics.

Figure 12.2D shows that the *RI* gives rise to a change in the slope (stiffness) of the *IC*. The initial angle θ coincides with a threshold angle defined by $\lambda_1 + \lambda_{12}$. This threshold angle is composed of two components: λ_1 associated with central commands and λ_{12} with *RI*. Let the joint angle increase quasi-statically from θ to θ'' through θ^3. If the inhibitory effect (λ_{12}) were fixed, the flexor torque would increase according to the *IC* (thin solid line) specified by threshold $\lambda_1 + \lambda_{12}$. However, in fact, the inhibitory effect on the flexor *MN*s decreases as θ increases and the extensor shortens. This displaces the flexor *IC* to the left (Figure 12.2D, dashed lines). As a consequence, torques T^3 and T'' are generated. This results in a steeper muscle characteristic (thick solid line) than would occur in the absence of *RI*. The same effect occurs for the extensor muscle. Thus, *RI* acts to modulate the positional gain (stiffness) of the system as has been suggested (Nichols, 1989). Therefore, increases in stiffness need not be attributed to the autogenic stretch reflex. The influence of *RI* on stiffness under static conditions (i.e., $dx/dt = 0$) can also be shown analytically:

$$\begin{aligned} dA_1/d\theta &= d(\theta - \lambda_1 - \lambda_{12})/d\theta \\ &= 1 - d\lambda_{12}/d\theta \end{aligned} \tag{12.11}$$

where λ_{12} is an increasing function of antagonist spindle afferent activity S_2 and a decreasing function of θ. As a result $dA_1/d\theta > 1$, i.e., the gain of the system with *RI* exceeds that of the system without *RI*.

It is of interest to consider the role of *RI* when a *C* command acts. To do so, we used a simple model based on *Eq. 12.10* for static conditions with linear dependencies of λ_{12} and λ_{21} on spindle afferent activity S_2 and S_1, respectively. Figure 12.2E and 2F show *IC*s when *RI* was either absent (2E) or present (2F). *RI* can influence the slope of the total *IC* by changing the size of the coactivation zone and the slope of the *IC*s of individual muscles. By comparison, without *RI*, the central *C* command affects the system's gain only by changing the size of the coactivation zone (Figure 12.2C).

The *RI* also affects reflex damping which characterises the ability of the system to change muscle activity as a function of velocity. In the absence of *RI*, this component of damping is equal to μ. When *RI* acts, the afferent component of damping is:

$$dA_1/d\omega = d(\theta - \lambda^*_1 - \lambda_{12})/d\omega = \mu - d\lambda_{12}/d\omega > \mu \qquad (12.12)$$

The inequality is justified by the fact that λ_{12} is an increasing function of extensor spindle afferent activity S_2 whereas S_2 is a decreasing function of angular velocity ω.

12.3.2 Renshaw Cells (RCs) in the Inter-Muscular Interaction

Agonist *RC*s inhibit the *Ia* interneurons that inhibit antagonist *MN*s (Figure 12.2A). This disinhibitory effect will be expressed as a change in the antagonist λ. For example, the effect elicited by extensor *RC*s on flexor *MN*s is denoted by λ_{12}'. This shift for flexor muscles is negative, its absolute value increases if extensor activity A_2 increases. A_2, in turn, is a decreasing function of θ. The effect of *RC* on the individual and total *IC*s is opposite to the effect of *RI*. Using the same analysis described above for *RI*, it can be shown that *RC* reduces the slopes of the individual and total *IC*s. On the whole, both *Ia IN*s and *RC*s are likely to belong to the system which establishes appropriate values of stiffness and damping.

12.3.3 Mutual Facilitation of Synergists

Ia afferents of muscle spindles terminate on both homonymous and heteronymous *MN*s. This gives rise to a steeper *IC* for each of the synergist muscles than would be the case in the absence of the facilitatory interaction. The considerations are similar to those used for the estimation of *RI* effects (Figure 2E). When a flexor muscle is stretched from a threshold angle, *Ia* afferents of synergist muscles give rise to a decrease in the flexor threshold angle. As a result, the *IC* which represents autogenic afferent effects shifts to the left so that the slope of the muscle torque-angle relationship is steeper than in the absense of the facilitatory interaction.

12.3.4 *RI* and *RC* Central Commands

Both *Ja IN*s and *RC*s are effectively controlled by descending systems. We associate this action with the occurrence of independent central commands. How can these commands be expressed in terms of the λ model? By analogy with the *MN*, the threshold membrane potential of an *Ia IN* and its recruitment occur at a specific joint angle. An independent central action on *Ia IN*s (we call this action the *RI* command) can be measured by a decrement or an increment of the threshold angle. Similarly, central *RC* commands specify the membrane potentials of Renshaw cells. As a result, the inhibitory action of *RC*s can be associated with a specific threshold level of muscle activity.

Thus, the *RI* command allows the nervous system to specify the angular range in which stiffness and damping will be enhancened whereas the *RC* command specifies the range of muscle activation in which the *RI* action is attenuated.

12.4 Muscle Torques: Hill Force-Velocity Relation

The dependence of muscle force on velocity (e.g. see Chapters 1, 5) reflects the mechanism of attachment and detachment of actin-myosin cross-bridges (Descherevsky, 1977). The force-velocity relation has usually been studied under conditions of constant electrical stimulation of the muscle. It is a non-trivial problem to apply this relation to a muscle in vivo with varying activity. Within the framework of the λ model, we offer the following solution. Hill's equation will be represented in

terms of muscle torque and angular velocity and refer only to the contractile component of the muscle. We represent the equation for torque (T) in the general form:

$$T = h\,(P_o, \omega_c) \tag{12.13}$$

where ω_c is the velocity of the contractile (c) component, h is an increasing function of ω_c; P_o is isometric torque specified by muscle activation. Note that $h(P_o,0) = P_o$ and shortening is considered negative. For a combined consideration of flexor and extensor muscles, it is convenient to transform muscle length into joint angle θ. Furthermore, θ can be decomposed into contractile (c) and series (s) elastic components such that $\theta = \theta_c + \theta_s$. Then we find $\omega_c = d\theta_c/dt$.

To solve *Eq. 12.13*, it is necessary to consider the series elastic component, which is assumed to have a spring-like characteristic:

$$T = g\,(\theta_s) \tag{12.14}$$

In addition, it is necessary to specify the isometric torque P_o as a function of muscle activation, A. This will be done in several steps. Under static conditions, P_o represents the muscle torque. Thus, P_o is a function of muscle activation, $P_o = f(A)$, where the function f describes the muscle *IC* and $A = \theta - \lambda$. Strictly speaking, A in this equation is static tonic activation. However, the dynamic muscle activation, $A = \theta - \lambda^*$ is equivalent to the static activation, $A = \theta - \lambda\hat{I}$, if the static threshold, $\lambda\hat{I}$, is numerically equal to the dynamic threshold, λ^*. Consequently, the equation $P_o = f(A)$ represents isometric muscle torque irrespective of whether the muscle activation A is static or dynamic and *Eq. 12.9* and $P_o = f(A)$ can be used to find P_o.

Note that the active state, P_o, for a given level of activation, sets in gradually with a time constant. Thus we assume that an additional time-dependent transformation plays a role in the above relation so that:

$$D\,(P_o) = f(A) \tag{12.15}$$

where D is assumed to be an operator of the second order:

$$D\,(P_o) = (1 + \tau_1\, d/dt + \tau_2^2\, d^2/dt^2)\, P_o \tag{12.16}$$

The time constants, τ_1 and τ_2, characterize the calcium-dependent proceess of the excitation-contraction coupling.

To make the above relations complete, an equation of motion has to be specified. In addition, it is necessary to specify the timing of central commands. For single joint movements the equation of motion has the form:

$$I\, d\omega/dt = T_2 - T_1 + L \tag{12.17}$$

where T_1 and T_2 are muscle torques, L is an external load (e.g., gravitational torque), and I is the inertia of the movable part of the system distal to the joint. In the double-joint model, Newton-Euler equations of motion were used (e.g., Hollerbach and Flash, 1982).

12.5 Timing of Central Commands for Single Joint Movements

It has been suggested in terms of the λ model (Feldman, 1979; Adamovich and Feldman, 1984) that the brain can specify the velocity and duration of changes in the R command and thus indirectly controls basic kinematic characteristics of movements (speed, duration and magnitude). This hypothesis has been corroborated for movements performed at moderate speeds (Abend et al., 1982)[1] and fast movements (Adamovich et al., 1984).

Figure 12.3A shows a scheme of the formation of the R command for stereotyped point-to-point single-joint movemements realized on a computer λ model. The R command is assumed to result from the summation of individual components each of which produces an elementary shift, R_i, in the equilibrium position. The movement distance is specified by the number of elementary components the brain issues. A priori, the components can be activated either successively (Figure 12.3A, input 1) or simultaneously (input 2). In the case of successive activation, the R command will shift gradually to its final value. The rate of shift

[1] Abend et al. (1982) concluded that there is a gradual shift in the equilibrium position for point-to-point movements. This conclusion is quite consistent with the λ model but not with the α model the authors suggest. In the α model, shifts in equilibrium are assumed to be a consequence of changes in muscle activation. Consequently, a gradual shift in equilibrium must be associated with a monotonic change in flexor and extensor *EMGs*. This is not consistent with experimental data showing that non-monotonic, three-burst *EMG* patterns are typical for these movements.

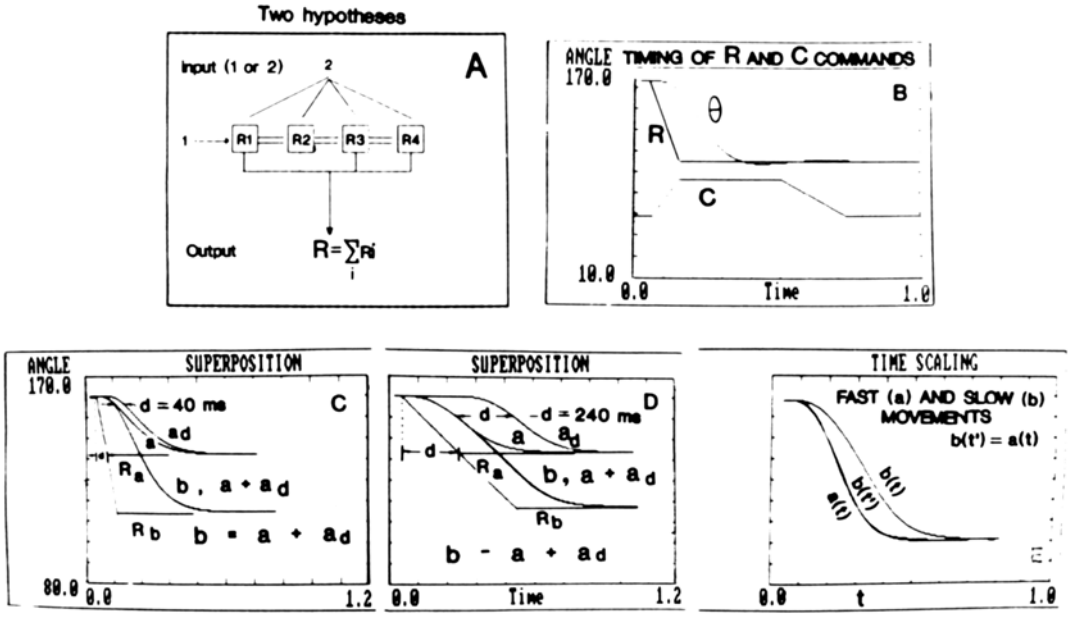

Figure 12.3: Properties of central commands and resulting movements in the λ model. *A)* Hypothetical components (R_i) of the R command. In scheme 1, the components are activated sequentially. In scheme 2, they are activated in parallel. Scheme 1 is consistent with experimental data and was used in the model. *B)* Typical form of R and C commands for fast active movements in the model (θ is joint position). *C, D)* Examples of verification of the principle of superposition for fast (C; dR/dt = 600°/s) and slow (D, 60°/s) movements. *E)* Demonstration of time scaling for movements of the same amplitude.

depends on the time interval between successive activations and can be centrally controlled. If the rate of shift is constant for a set of successively generated movements, but the duration varies, then the movement paths will initially be the same and then will diverge as a function of distance. However, if the rate of shift, and consequently torque, varies then the trajectories will deviate from each other from the very beginning. In constrast, in the case of simultaneous activation, only the amplitude of the shift, but not the rate of shift, can be controlled. The amplitude of shift will depend on the number of simultaneously activated units. The fact that the trajectories of single-joint fast movements coincide at an initial phase (Wadman et al., 1979; Adamovich et al., 1984) is consistent with the hypothesis of successive summation of command components. In addition, the successive model can account for experimental movements in which the paths diverge from the very beginning (cf. Chapter 14 (Gottlieb et al.)).

The C command and other central commands can be graded in a similar way and may be used either in combination with the R command or in isolation, depending on motor tasks. For example, the C command can be set before the movement initiation produced by the R command.

Figure 12.3B shows a hypothetical time course of the R and C commands used in the model for stereotyped one-joint point-to-point movements. The commands gradually change at constant speeds until the necessary final values are reached. The values as well as the speeds are controlled variables. The fastest movements are associated with the maximal values of rate of shift of central commands. After the end of the movement the final R command remains constant but the C command gradually diminishes: the first provides the final equilibrium position and has to be sustained whereas the higher stiffness of the joint the C command creates is necessary only during the movement and after its end the C command may be reduced. The magnitudes and speeds of the R and C commands may be correlated, especially for fast movements. However, this need not be the case. For example, a constant C command can be specified before the movement and remain during the movement.

12.6 The Principle of Superposition and Time Scaling

The hypothesis that gradual constant-rate control signals underlie stereotyped one-joint movements has numerous consequences. Figures 12.3C and D show a computer test of one of them, the principle of superposition. In 3C, two position-time functions, a and b, were elicited by R_a and R_b commands having the same speed (–600°/s) but R_b was twice the duration of R_a. The duration of their common path was 40 ms. Movement a was shifted to the right at time = 40 ms and denoted a_d. Summation of a and a_d resulted in the curve $a + a_d$ that coincides with movement b. The same is true for movements performed at a slow command speed (–60°/s, Figure 12.3D). In general, a single movement trajectory having distance $n\ a$ can be split into n identical trajectories of distance a and generated one after another with a time delay that is equal to the duration of the common path of the large and small movements. The only constraint is that the velocity of the R commands underlying the movements must be the same whereas the rest of the central commands may remain constant or vary as a single-valued function of the R command duration.

The principle of superposition has experimentally been verified for $n = 5$ and used to measure the rate (500–700°/s) of the R command for fast point-to-point movements (Adamovich et al., 1984; Abdusamatov et al., 1987).

Another advantage of constant velocity control signals is that a simple modification of the control velocity provides scaling of movements in time (Figure 12.3E). This is consistent with experimental data. In addition, R commands having an equal duration but different velocities give rise to movements that can be superimposed by scaling in amplitude. For discussions of movement scaling see Schmidt (1982), Chapter 14 (Gottlieb et al.) and Chapter 19 (Seif-Naraghi and Winters).

12.7 Movement Corrections

One more interesting consequence of the constant-velocity form of the control signals concerns corrections of movements in response to an unexpected shift of the target. Provided the new target position is not presented too late, the sweeping of the control signal can be stopped earlier or continued further depending on the new target position. The movement kinematics would be the same as a movement initially planned to the final target, and there will be no inflection point in the movement trajectory. This effect has been demonstrated for both arm and eye movements (Pellisson et al., 1986). (The simultaneous model discussed in Section 12.5 cannot account for these findings.) Note that the rate of the control signals in movements in which a final position must be reached very precisely may be slowed down while the arm is approaching the target.

12.8 Wave Command Generator

The neuronal organization of the brain structures underlying central commands is not known. The wave hypothesis proposed earlier (Adamovich et al., 1984) and described below is one simple possibility. The R command is assumed to be graded by a hypothetical segmental or suprasegmental neuronal ensemble arranged sequentially. Higher brain levels specify constant tonic influences on the ensemble during some time. The amplitude of the tonic signal specifies the rate of propogation of excitation along the neuronal ensemble. This causes new neurons of the ensemble to become tonically active, and these neurons discretely contribute to the R command. The number of neurons recruited is associated with the value of R and the final value of R will depend on the duration of the tonic control signal and its amplitude. The discrete neuronal activations result in individual movements which sum up successively according to the superposition principle. Similar wave structures may be associated with the C and other central commands.

12.9 Single-Joint Movements: EMGs and Kinematics

For simulations of single joint movements, we used λ models of different complexity. In a minimal model, the concepts of *MAA*, *IC*, *R*, and *C* central commands with appropriate timing, and Newton's equation of motion were used. However, this model did not include Hill's force-velocity relation and intermuscular interactions mediated by muscle afferents. It was essential to demonstrate that even such a simplified model qualitatively reproduces typical *EMG* patterns and basic kinematic characteristics of single joint movements including the three-burst *EMG* pattern typical of fast point-to-point

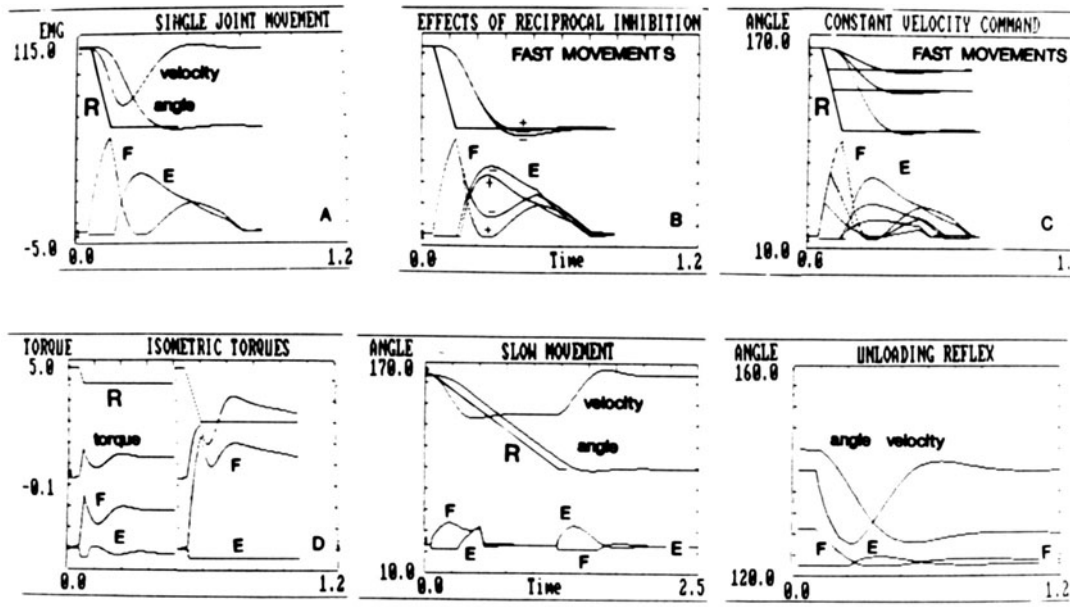

Figure 12.4: Flexor (*F*) and extensor (*E*) activation patterns ("*EMG*s") and kinematics in the model for single joint movements. (See text for details.)

movements. In more complex models, a linear approximation of the Hill force–velocity relation, series elastic and contractile muscle components, and reciprocal interaction between antagonist muscles were used. These additional properties of the system improve somewhat the characteristics of performance but do not change them radically. The value of the reflex damping parameter μ ranged between .05 and .12 *s*. This range encompassed both overdamped and underdamped motions.

12.9.1 Fast Active Movements

Figure 12.4A-C shows typical simulated *EMG* patterns for fast point–to–point movements. The calculations were made with the use of the minimal model (Figure 12.4B, curves with "–") and the model that included the reciprocal interaction between antagonist muscles and the Hill force–velocity relation (Figure 12.4B, curves with "+" and Figures 12.4A and C). A tri-phasic pattern of *EMG* is especially pronounced if there is a reciprocal interaction between antagonist muscles (compare "+" and "–" in B). This is independent of movement amplitude (Figure 12.4C). It should be emphasised that this pattern results from a constant velocity control signal *R* (600°/s). The resulting movement has a bell-shaped velocity profile (Fig. 12.4A) which is typical for actual movements (Chapter 14 (Gottlieb et al.)). The dependence of the amplitude of the agonist and antagonist burst activity on movement amplitude (Figure 12.4C) is also consistent with experimental data (Brown and Cooke, 1981; see also Chapter 14).

12.9.2 Isometric Torques

In isometric conditions, the same central commands as in Figure 12.4A–C give rise to a fast increase in the agonist muscle torque (Fig. 12.4D). In this model, a series elastic component and a contractile muscle component with a linear dependence of force on velocity were included. For a fast torque production of moderate magnitude (left panel), a bi-phasic *EMG* pattern with reciprocal activation of agonist and antagonist muscles was observed (cf. Gordon and Ghez, 1984). The antagonist muscle activity was totally suppressed in the case of fast torque generations of large magnitudes (right panel).

12.9.3 Active Movements at Moderate Rates

The rate of change of the R command was diminished to about 60°/s to produce movements having a moderate speed. The C command was correspondingly attenuated. As a result, after a short period of acceleration the arm moves at a constant velocity (Figure 12.4E). The movement ends soon after the R command reaches its final value. In contrast, fast movements last relatively long after the end of control signals (cf. Figure 12.4A). During large movements at a moderate rate, the muscles are active in the initial and terminal phases of the movement whereas in the intermediate phase, when the velocity is constant, they are not active at all (Figure 12.4E) (Cooke and Brown, 1990).

12.9.4 Unloading Reflex

The effects of perturbations during posture and movements may be tested with the λ model. As an example, Figure 12.4F shows a simulation of *EMG*s and kinematics in the case of an abrupt unloading of the agonist muscle with constant R and C commands. The model reproduces characteristic features of the unloading reflex if the subject is instructed not to correct the deflections of posture (Feldman, 1986): a silent period in the agonist *EMG*, a transfer of the arm to a new position, and a lower level of tonic *EMG* corresponding to the residual load after the end of movement.

12.9.5 Rhythmic Movements

In the λ model, active rhythmical movements can be elicited in different ways. First, a central generator can produce rhythmical changes in the R command. The other commands can either remain constant or be changed in-phase with the R command. *EMG* can arise, indirectly, from changes in central commands. However, *EMG* responses may also arise rapidly from perturbations during movement while the form of the central commands remains unchanged. The phase of oscillations remains the same in spite of perturbations. Second, rhythmical movements can be received when central control signals remain constant and there is strong coactivation in combination with a high gain for the reciprocal interaction between antagonist muscles. This produces alternative activation of antagonist muscles. The movement amplitude of the limb can be controlled by the coactivation and reciprocal inhibition commands and the midpoint of the movement range is specified by the R command. Activation and deactivation of antagonist muscles are locked to specific positions of the limb. The period of the oscillation depends on the inertia of the limb. If the limb is arrested, tonic activity in the agonist muscle is established and the oscillations cease. If the limb is released, the oscillations resume with a phase shift equal to the duration of the pause. Thus, the generator has some features reminiscent of that for slow walking (Grillner, 1975).

12.10 Double-Joint Movements: Control Signals, EMGs, and Kinematics

We have examined two-joint point-to-point arm movements using a double-joint model based on all the equations described above, where λ^* is given by *Eq. 12.4*. The model includes six muscles: single-joint flexor and extensor muscles for each joint and double-joint flexor and extensor muscles. Thus, the number of muscles is redundant. We consider first some properties of double-joint muscles in terms of the λ model and then suggest a strategy for the coordinative control of single- and double-joint muscles.

12.10.1 Double-Joint Muscles

The double-joint flexor muscle length is, to a first approximation, a linear function of the two joint angles, θ_1 and θ_2:

$$x = a\,\theta_1 + b\,\theta_2 + c \qquad (12.18)$$

where coefficients are positive. We define a weighted angle, θ:

$$\theta = p\,\theta_1 + q\,\theta_2 \qquad (12.19)$$

where $p + q = 1$ and $p = a/(a + b)$. There is a single-valued correspondence between this angle and the muscle length: $\theta = (x - c)/(a + b)$. The sense of this is that the length $x - c$ is considered as an arc of a circle having the radius $a + b$. The angle corresponding to this arc is θ. The same rule is used for transformation of the threshold length of each double-joint muscle into an angular one, λ. As a result, the condition of activation for the double-joint flexor muscles has the form:

$$\lambda - \theta \geq 0 \qquad (12.20)$$

which is similar to that for single joint flexor muscles.

For double-joint muscles, the R and C commands are defined as for single joint muscles but in terms of weighted thresholds. Thus, we consider commands R_1 and R_2 for the single and R for double-joint muscles. A given value of R is associated with an equilibrium value of weighted angle $\theta = R$. According to *Eq. 12.19*, a given value of the threshold angle can be achieved by different combinations of joint angles. It follows that central control signals to double-joint muscles provide a certain relation between equilibrium joint angles but not their specific values. Within the limits of this relation, the arm can go from one equilibrium combination to another in response to perturbations (indifferent equilibrium). In contrast, control signals R_1 and R_2 for single joint muscles provide a specific equilibrium configuration of the arm. For correspondence between the equilibrium positions specified by single- and double-joint muscles, the control signal R is established in accordance with *Eq. 12.19*:

$$R = pR_1 + qR_2 \tag{12.21}$$

12.10.2 General Scheme of Performance

A hypothetical scheme for the performance of reaching movements may be described as follows. There is a neuronal analog of the subject's external space in the sense that activation of a neuronal population localized about a point in the neuronal structure is associated with a point (X,Y) of the external space. In particular, this point can coincide with the position of the arm endpoint. When a target is presented to the subject, the localisation of the neuronal activity changes, and, correspondingly, the equilibrium position of the arm endpoint shifts in the external space in the direction of the target. We assume that this shift in equilibrium, if there are no special constraints, occurs along a straight line at a constant velocity until the target is reached. This control signal is then transformed into commands for each joint (R_1, R_2 and the double-joint R command) to elicit an actual movement to the target.

12.10.3 Equilibrium Spaces

To make the above representations more precise, we define two neuronal spaces in the λ model. The first is the space of equilibrium end point positions corresponding to actual end point positions. We call this notion the equilibrium space (*ES*). The second is the space of equilibrium joint configurations which represents all possible combinations of control signals R_1 and R_2. Assuming equal link lengths, m, for the double-joint arm, the transformation between equilibrium joint space and *ES* is:

$$\begin{aligned} X' &= m \sin R_1 - m \sin (R_1 + R_2) \\ Y' &= m \cos R_1 - m \cos (R_1 + R_2) \end{aligned} \tag{12.22}$$

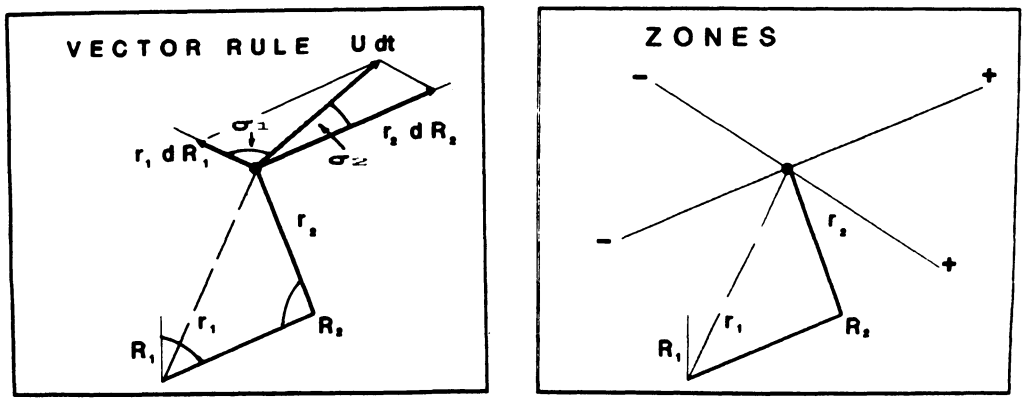

Figure 12.5: Relationship between the end point and joint control signals. Left panel: the end point displacement vector $U\ dt$ can be decomposed into endpoint displacements ($r_i\ dR_i$) due to rotations of individual joints. r_1 and r_2 are the radial vectors at the shoulder and elbow. R_1 and R_2 are the central commands for these joints. Right panel: four zones of inter-joint coordination. The boundary line (with negative slope) orthogonal to radial vector r_1 corresponds to shoulder motion. Flexion is $-$. The other boundary line (orthogonal to r_2) is associated with elbow motion.

Here X' and Y' are the coordinates of the end point of the limb in *ES*. Since R_1 and R_2 are specified by the brain and since the form of the above transformation also describes the relation between actual end point and joint coordinates, the *ES* is an isomorphic representation of external space. The brain produces movements by specifying a velocity vector, U, based on the *ES*. The effect is tantamount to a shift in the equilibrium position of the end point in the actual external space.

Given a goal-directed vector U, it is necessary to specify individual commands for each joint. They must be coordinated in such a way that the vector summation of the displacements of the end point elicited by rotations in each joint together give the desired vector U (Figure 12.5, left panel). The displacement of the end point due to rotation in the *i-th* joint equals the vector product of the radial vector r_i directed from the axis of the joint to the end point and the vector of rotation dR_i. Thus:

$$\Sigma\, r_i\, dR_i = U\, dt \qquad (12.23)$$

Eq. 12.23 applies to systems with any number of links as well as two- and three-dimensional motion. For double-joint limb and two-dimensional space the equation can be solved for R_i:

$$dR_1/dt = -a_1\, U \sin \sigma_2 \qquad (12.24)$$

R_2 is obtained by transposing subscripts *1* and *2*. In *Eq. 12.24*, U is the length of the velocity vector, σ_2 is the angle between the vector U and the displacement of the end point due to rotation of the second joint (Figure 12.5, left panel), $a_1 = 1/r_1 \sin(\sigma_1 - \sigma_2)$ depends only on the current configuration of the limb but not on the direction of the vector U. *Eq. 12.24* shows that the control signal for one joint depends on the parameters of the other joint. This strategy is different from that suggested by Berkinblit et al. (1986).

Thus, several levels of motor control are suggested in the λ model. At a high neuronal level, a constant-velocity vector U is specified that corresponds to the direction and rate of the shift in the equilibrium position of the end point. The signal is then transformed into individual commands for each joint and the movement is realized according to the λ model. Indeed, both the magnitude and direction of U can be modified in the course of movement to correct errors, to accelerate or decelerate the movement, to react to a sudden change in the target position, or to avoid obstacles. Otherwise, if there are no special constraints, the velocity vector remains constant until the target is reached.

The λ model gives a realization of the scheme of motor control suggested by Georgopoulos et al. (1988) [see also Chapter 16 (Hasan and Karst) and Chapter 17 (Flash)] in their study of motor cortex neuronal activity. We can associate the population vector in their study with vector U in the λ model. In addition, *Eq. 12.24* shows that, for any configuration, the control signal is maximal when $\sigma_2 = 90°$. The control signal will be a cosine function of the angle between this optimal direction and the actual movement direction. The corresponding dependence is characteristic of cortical neurons. This allows us to suggest that motor cortex neurons convey information about the target vector U as well as the individual central commands that produce shifs of the equilibrium for each joint.

12.10.4 Velocity Profiles and *EMG*s

Numerous studies have shown that the end point velocity profile in point-to-point arm movements is typically bell-shaped [e.g., see Chapter 17 (Flash)]. According to the λ model, movements are smooth because of the system's natural dynamics [see also Chapter 19 (Seif-Naraghi and Winters)]; the brain does nothing to produce a smooth movement [cf. Chapter 11 (Hogan), Chapter 17 (Flash)]. Figure 12.6 demonstrates that the λ model, with constant velocity shifts in the equilibrium position of the end point, is able to produce a bell-shaped velocity profile of the actual movement of the end point as well as the individual joints.

The magnitude and duration of *EMG*s in the model are a function of movement direction (Figure 12.6A,B). In the absence of joint movement reversals, agonist-antagonist patterns of *EMG* are tri-phasic.

Figure 12.5 (right panel) shows four zones relating movements of the end point to the directions of joint motion. Within each zone, joint motion directions (e.g., ++) remain constant. Joint reversals occur when the direction of U changes from one zone to another. The borders between zones are defined by the equation $\sin(\sigma_i) = 0$ (see

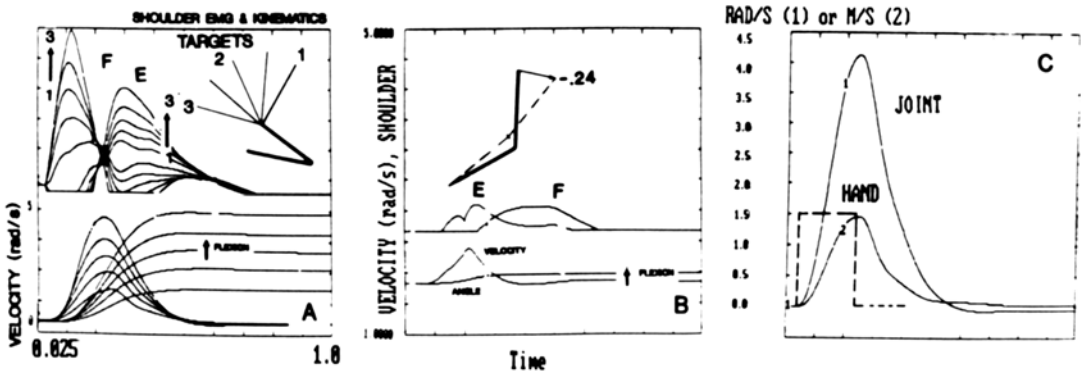

Figure 12.6: Shoulder EMG patterns and kinematics in the double-joint model. The numbers in A and B indicate movement direction (*rad*). ***A, B)*** Movements without joint reversals. ***B)*** A movement near to the border between zones shown in Figure 12.5, right panel. Note that the extensor is active first during flexor movement. ***C)*** Bell-shaped end point tangential and joint velocity profiles. Notice that a constant-velocity control signal (dashed line) underlies these movements.

Eq. 12.24; see also Chapter 16 (Karst and Hasan). Near the boundaries of the zones the model can produce *EMG* patterns that are counter-intuitive. For example, the beginning of flexor movement can be associated with an initial extensor *EMG* as has been shown experimentally (Hasan & Karst, 1989; Chapter 16). Bernstein (1967) has also described rather widespread cases when the movement direction is opposite to what we could predict based on the *EMG*s. Reactive forces and other dynamic effects in multi-joint systems may also affect the relations between *EMG*s and movement kinematics.

12.11 Double-Joint Movements: Corrections and the Principle of Superposition

The principle of superposition formulated above for one-dimensional control signals and resulting movements can be generalized to multi-dimensional performance. We have suggested that the control signal which is specified at the level of the *ES* is a vector. As a consequence, the vector can be decomposed in a sum of two or more components. For example, in case of an orthogonal decomposition we have:

$$U = U_x + U_y \tag{12.25}$$

It is suggested that the corresponding decomposition is also possible for the resulting movement.

In this connection it is interesting to apply the principle of superposition to movement corrections in response to a sudden shift of the target. This paradigm has been used by Flash (Chapter 17) with another model based on control signals with bell-shaped velocity profiles. In our model, there is a single control vector, U, which may be modified (in both magnitude and direction) in response to a shift in target position. On the other hand, we may assume that the old control signal is not interrupted and a new control signal is added. The new signal, V, is directed from the old target to the new target (Figure 12.7). Within the framework of the λ model the two strategies are formally equivalent and the resulting movements may coincide.

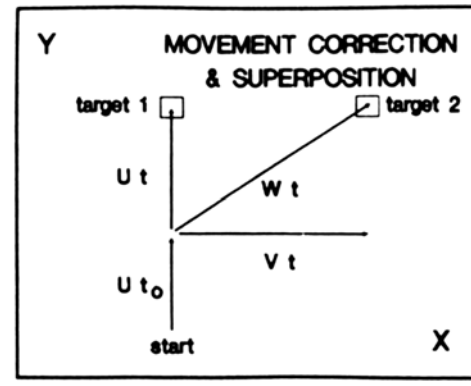

Figure 12.7: Movement corrections and the principle of superposition in a vector formulation of the control processes for multi-joint movements. (See text for details.)

In the model developed by Flash (Chapter 17), control signals are bell-shaped. To form them the nervous system has to estimate beforehand movement distances. In the case of movement correction, the old control signal continues simultaneously with the new correction signal. In constrast, our model assumes a single constant velocity control signal. Thus, the nervous system need not specify movement amplitude in order to initiate movements and reserves the possibility to specify or correct the final equilibrium position of the end point during the course of the movement depending on the current situation.

12.12 The Redundancy Problem

If the number of joints exceeds the dimension of external movement space and its inner, *ES* model, the solution of *Eq. 12.23* is ambiguous, i.e., the system is redundant (see also Chapters 6-11, 16-22). If there are no additional constraints (e.g., those limiting possible coordinations of control variables), the brain can apply one or another optimal control strategy to issue concrete commands. One solution to *Eq. 12.23* is to find commands $d\boldsymbol{R}_i/dt$ which give rise to a vector $\boldsymbol{U}'$ having a least square deflection from the desired vector $\boldsymbol{U}$. With this constraint, a solution of *Eq. 12.23* can be found with the use of the method of the pseudo-inverse matrix (Gantmaher, 1966; cf. Mussa Ivaldi et al., 1988). Thus, the commands will be minimal in the sense of their "energy" (Gantmaher, 1966):

$$\S\,(d\boldsymbol{R}_i/dt)^2 = \text{minimum} \qquad (12.26)$$

This solution of *Eq. 12.26* could, in principle, be found through dynamic neuronal interaction between and within the end point and joint equilibrium spaces. This interaction gives rise to control signals which minimize the movement deflection from the target vector $\boldsymbol{U}$ (*Eq. 12.23*) which, in turn, minimizes the "energy" of control signals in the sense of *Eq. 12.26* [see also Chapter 19 (Seif-Naraghi and Winters) for a similar approach based on dynamic optimization].

12.13 Conclusions and Future Directions

We have illustrated several ideas and conceptions which seem essential for the understanding of motor control and performance. First of all, it is necessary to find an adequate measure of the action of brain control structures on motoneuronal pools which is independent of kinematic variables characterizing the state of the periphery. This action is associated with the voluntary control of both posture and movement. In this analysis the threshold properties of *MN*s have been taken into account. The control signals are manifest in a change in the threshold length, λ, at which motoneurons become recruited. The λ is an experimentally measurable variable (Feldman, 1986). One more concept - the muscle activation area - is essential in the explanation of *EMG*s and the kinematics and dynamics of single- and double-joint movements. Intermuscular interactions have also been described in terms of the λ model. Importantly, according to the λ model, muscle activities, forces, and movement kinematics need not be iteratively calculated over the course of movement.

We have also illustrated the notion that each level of motor control may be associated with a specific invariant variable and performs specific motor functions (cf. Bernstein, 1967). In particular, a constant value of the parameter $\boldsymbol{R}$ is associated with the postural control of the joint. In this case, the system can generate responses to perturbations and a new equilibrium position will be established if the external load changes. The invariance of the target vector, $\boldsymbol{U}$, produces an active directional movement of the arm endpoint. The level $\boldsymbol{U}$ does not exclude the behavior associated with the level $\boldsymbol{R}$ but may modify the behavior.

We offered various formulations of the principle of superposition both for control signals and resulting movements. Usually, principles of superposition are considered a characteristic of linear systems. The λ model is thus an example of linear behavior of the system in spite of nonlinearity of its single components. This does not mean that we can neglect nonlinearities.

It is a characteristic of the λ model that it combines both biomechanical and neurophysiological notions. The biomechanical aspects of the λ model can be developed by combining it with equations of the chemical kinetics of muscle contraction (Feldman, 1979). The neurophysiological aspects of the λ model allows us to explain different *EMG* patterns. Potentially, neurophysiological elements of the λ model can be modelled using neuronal nets (e.g., Chapter 20 (Denier van der Gon et al.). In this case, the λ model may be coordinated with experimental data concerning the activity of neurons in the motor cortex and other brain structures.

References

Abdusamatov R.M., Adamovich S.V., Berkinblit M.B., Chernavsky A.V. and Feldman A.G. (1988) Rapid one-joint movements: a qualitative model and its experimental verification. In *Stance and Motion: Facts and Concepts* (Eds. Gurfinkel V.S., Ioffe M.E., Massion J. and Roll J.P.), Plenum Press, New York, pp. 261-270.

Abdusamatov R.M., Adamovich S.V. and Feldman A.G. (1987) A model for one-joint motor control in man. In *Motor Control.* (Eds. Gantchev, G., Dimitrov, B. and Gatev, P.), Plenum Press, New York, pp. 183-188.

Abdusamatov R.M. and Feldman A.G. (1986) Description of electromyograms by a mathematical model of single joint movements. *Biofizika* **31**: 503-505.

Adamovich S.V., Burlachkova N.I. and Feldman A.G. (1984) Wave nature of the central process of formation of the trajectories of change in joint angle in man. *Biophysics* **29**: 130-134.

Abend W., Bizzi E. and Morasso P. (1982) Human arm trajectory formation. *Brain* **105**: 331-348.

Adamovich S.V. and Feldman A.G. (1984) Model of central regulation of the parameters of motor trajectories. *Biophysics* **29**: 338-342.

Baldissera F., Hultborn H. and Illert M. (1981) Integration in spinal neuronal systems. In *Handbook of Physiology, Sec. 1, Vol. II, The Nervous System: Motor Control, Part 1,* (Ed. Brooks, V.B.), Williams and Wilkins, Baltimore, pp. 509-595.

Bernstein N.A. (1967) *The Coordination and Regulation of Movements.* Pergamon Press, London.

Berkinblit M.B., Gelfand I.M. and Feldman A.G. (1986) A model for the control of multi-joint movements. *Biofizika* **31**: 483-488.

Bizzi E. (1980) Central and peripheral mechanisms in motor control. In *Tutorial in Motor Behavior* (Eds. Stelmach G.E and Requin J.), North-Holland, Amsterdam, pp. 131-144

Brown S.H. and Cooke J.D. (1981) Amplitude- and instruction-dependent modulation of movement-related electromyogram activity in humans. *J. Physiol.* **316**: 97-107.

Burke R.E., Rymer W.Z. and Walsh J.V. (1976) Relative strength of synaptic input from short-latency pathways to motor units of defined type in cat medial gastrocnemius. *J. Neurophysiol.* **39**: 447-458.

Cooke J.D. & Brown S.H. (1990) Movement related phasic muscle activation. II: Generation and functional role of the tri-phasic pattern. J. Neurophysiol. 63: 465-472.

Descherevsky V.I. *(1977) Mathematical Models of Muscle Contraction.* Nauka, Moscow, pp. 1-160.

Feldman A.G. (1974) Control of the length of a muscle. *Biophysics* **19**: 776-771.

Feldman A.G. (1979) *Central and Reflex Mechanisms in Motor Control.* Nauka, Moscow, pp. 1-184.

Feldman A.G. (1980) Superposition of motor programs. II. Rapid forearm flexion in man. *Neurosci.* **5**: 91-95.

Feldman A.G. (1986) Once more on the equilibrium-point hypothesis (< model) for motor control. *J. Mot. Behavior* **18**: 17-54.

Feldman A.G. and Orlovsky G.N. (1972) The influence of different descending systems on the tonic stretch reflex in the cat. *Exp. Neurol.* **37**: 481-494.

Feldman A.G. and Orlovsky G.N. (1975) Activity of interneurones mediating reciprocal Ia inhibition during locomotion in cats. *Brain Res.* **84**: 181-194.

Flash T. (1987) The control of hand equilibrium trajectories in multi-joint arm movements. *Biol. Cybern.* **57**: 257-274

Gantmaher F.R. (1966) *The Theory of Matrices.* Nauka, Moscow, pp. 1-576.

Georgopoulos A.P., Kettner R.E. and Schwartz, A.B. **(19XX)** Primate motor cortex and free arm movements to visual targets in three-dimensional space. II. Coding of the direction of movement by a neuronal population. *J. Neurosci.* **8**: 2928-2937

Gordon, J. and Ghez, C. (1984) EMG patterns in anatagonist muscles during isometric contraction in man: Relations to response dynamics. *Exp. Brain Res.* **55**: 167-171.

Grillner, S. (1975) Locomotion in vertebrates: central mechanisms and reflex interactions. Physiol. Rev. 55: 247-304.

Hasan Z. and Karst G.M. (1989) Muscle activity for initiation of planar, two-joint arm movements in different directions, *Exp. Brain Res.* **76**: 651-655.

Hogan N. (1984) An organizing principle for a class of voluntary movements. *J. Neurosci.* **4**: 2745-2754.

Hollerback, J.M. (1985) Computers, brains and the control of movements. *Trends in Neurosci.* **5**: 189-192.

Houk J.C. and Rymer Z.W. (1981) Neural control of muscle length and tension. In *Handbook of Physiology, Sec. 1, Vol. II, The Nervous System: Motor Control, Part I* (Ed. Brooks, V.B.), Williams and Wilkins, Baltimore, pp.257-323.

Hollerbach, J.M. and Flash, T. (1982) Dynamic interaction between limb segments during planr arm movement. *Biol. Cybern.* **44**: 67-77.

Hultborn H. (1972) Convergence of interneurons in the reciprocal Ia inhibitory pathway to motoneurones. *Acta Physiol. Scand., Suppl.* **375**: 1-42.

Lundberg A. (1975) Control of spinal mechanisms from the brain. In *The Nervous System, Vol. 2*, (Ed. Tower, D.B.), Raven Press, New York, pp. 253-265.

Mussa-Ivaldi F.A., Morasso P. and Zaccaria, R. (1988) Kinematic networks. A distributed model for representing and regulation of motor redundancy. *Biol. Cybern.* **60**: 1-16.

Nichols T.R. (1989) The organization of heterogenic reflexes among muscles crossing the ankle joint in the decerebrate cat. *J. Physiol.* **410**: 463-477.

Pellison D., Prablanc C., Goodale M.A. and Jeannerod M. (1986) Visual control of reaching movements without vision of the limb. II. Evidence of fast unconscious processes correcting the trajectory of the hand to the final position of a double-step stimulus. Exp. Brain Res. **62**: 303-311.

Schmidt R.A. *(1982) Motor Control and Learning: A Behavioral Emphasis.* Human Kinetic Publishers. Champaign, IL, pp. 303-326.

Soechting J.F. and Lacquaniti F. (1981) Invariant characteristics of a pointing movement in man. *J. Neurosci.* **1**: 710-720.

Viviani P. and Terzuolo C.A. (1982) Trajectory determines movement dynamics. *Neurosci.* **7**: 431-437.

Wadman W.J., Danier van der Gon J.J., Geuze R.H. and Mol C.R. (1979) Control of fast goal-directed arm movements. *J. Hum. Mov. Studies* **5**: 3-17.